Physiology & Behavior 214 (2020) 112760

Contents lists available at ScienceDirect

Physiology & Behavior

journal homepage: www.elsevier.com/locate/physbeh

Sleep profile during fasting in PPAR-alpha knockout mice

Yoshitsugu Kondo[a,b,1], Sachiko Chikahisa[a,1,*], Tetsuya Shiuchi[a], Noriyuki Shimizu[a], Daisuke Tanioka[a], Haruo Uguisu[b], Hiroyoshi Séi[a]

[a] Department of Integrative Physiology, Institute of Biomedical Sciences, Tokushima University Graduate School, Tokushima 770-8503, Japan
[b] Department of Physical Therapy, Faculty of Health and Welfare, Tokushima Bunri University, Tokushima 770-8514, Japan

ARTICLE INFO

Keywords:
PPARα
Sleep
Food deprivation
Ketone bodies

ABSTRACT

Peroxisome proliferator-activated receptor alpha (PPARα) is a transcription factor that belongs to the nuclear receptor family and plays an important role in regulating gene expression associated with lipid metabolism. PPARα promotes hepatic fatty acid oxidation and ketogenesis in response to fasting. Because energy metabolism is known to affect sleep regulation, manipulations that change PPARα are likely to affect sleep and other physiological phenotypes. In this study, we examined the role of PPARα in sleep/wake regulation using PPARα knockout (KO) mice. Sleep, body temperature (BT), locomotor activity, arterial pressure (AP) and heart rate (HR) were recorded in KO mice and wild-type (WT) controls under ad libitum-fed conditions and 24-hour food deprivation (FD). KO and WT mice were identical in basal sleep amount, BT, mean AP and HR, although KO mice showed enhanced sleepiness (enhanced EEG slow-wave activity). In response to FD, KO mice showed a large drop in wakefulness and locomotor activity at the end of the dark phase, whereas WT mice did not. Similarly, AP and HR, which were suppressed by FD, decreased more in KO than in WT mice. Compared to WT mice, KO mice showed a reduced concentration of plasma ketone bodies and decreased mRNA expression of the ketogenic enzyme gene *Hmgcs2* in the liver and brain under FD conditions. These results suggest that PPARα and/or lipid metabolism is involved in the maintenance of wakefulness and locomotor activity during fasting in mice.

1. Introduction

The peroxisome proliferator-activated receptor alpha (PPARα), one of three PPAR subtypes (α, β, and γ), is a ligand-activated transcription factor that regulates genes involved in lipid metabolism [1,2]. Similar to the action of other nuclear hormone receptors, PPARα activates transcription in response to ligand binding [3]. PPARα binds a peroxisome proliferator response element (PPRE) in the promoter region of target genes as a heterodimer with the receptor for *9-cis* retinoic acid, retinoid X receptor (RXR) [1]. The natural ligands of PPARα are fatty acids, and its synthetic ligands are fibrate drugs, which are used to treat hyperlipidemia [4]. PPARα is highest in the liver, followed by the kidney, heart, skeletal muscle, and brain [5]. PPARα in the liver controls the transcription of many genes involved in fatty acid metabolism, especially ketogenesis, in response to fasting [2,5]. Studies with PPARα knockout (KO) mice have revealed that PPARα plays a vital role in the biological response to fasting. For example, PPARα KO mice rapidly become hypoglycemic after food deprivation (FD) and cannot activate fatty acid oxidation and ketogenesis in the liver [6–8].

On the other hand, PPARα also plays an important role in many brain-related functions, including neuroprotection [9,10], control of neural stem cell activity [9], memory [11], fear learning [12] and sleep control [13,14]. We recently discovered that mice treated with bezafibrate, a PPARα ligand, showed enhanced slow-wave activity (SWA, power density of the electroencephalogram (EEG) delta band between 0.5 and 4.0 Hz in rodents, an indicator of sleep depth and sleepiness), in non-rapid eye movement (NREM) sleep [14]. Recently, we also found that sleep deprivation activated PPARα and ketogenesis in the brain, which may lead to enhanced SWA during NREM sleep [15]. These findings suggest that PPARα and ketone bodies play an important role in the regulation of sleep homeostasis.

As mentioned above, observations from many reports on PPARα emphasize its importance in responses to fasting [16]. Food restrictions, which are thought to activate PPARα, are known to affect sleep/wake patterns [17,18]. However, whether sleep changes during food restrictions are mediated by PPARα activity itself is unclear. Therefore, we investigated the role of PPARα in sleep/wake regulation during fasting using PPARα KO mice. We found that PPARα deficiency

* Corresponding author.
E-mail address: chika@tokushima-u.ac.jp (S. Chikahisa).
[1] These authors contributed equally to this work.

https://doi.org/10.1016/j.physbeh.2019.112760
Received 6 August 2019; Received in revised form 26 November 2019; Accepted 26 November 2019
Available online 27 November 2019

increased sleepiness at baseline and decreased wakefulness and locomotor activity, especially at the end of the dark (active) phase of the FD day. These sleep changes may be mediated by the alteration of lipid metabolism caused by PPARα deficiency.

2. Materials and methods

2.1. Animals

All experiments were performed using male PPARα KO mice (129S4SvJae-PPARαtm1Gonz/J, Jackson Laboratory, Maine, USA) and male WT mice originated from the littermates of PPARα KO mice. Eight-week-old mice were fed ad libitum and maintained on a 12-hour light-dark (L/D) cycle (lights on at 0900) at a controlled ambient temperature (23 ± 1° C). The total number of mice used in the experiment was 52, distributed as follows: baseline sleep recording, $n = 10$ (WT: $n = 5$, KO: $n = 5$); FD sleep recording, $n = 12$ (WT: $n = 6$, KO: $n = 6$); cardiovascular recording, $n = 6$ (WT: $n = 3$, KO: $n = 3$); biochemical analysis, $n = 24$ (WT: $n = 12$, KO: $n = 12$). The Animal Study Committee of Tokushima University approved these experiments (License No. T30-51), and we performed them in accordance with Guidelines for the Care and Use of Animals approved by the Council of the Physiological Society of Japan.

2.2. Surgery in preparation for sleep recording

Mice were anesthetized with a cocktail of ketamine (100 mg/kg) and xylazine (25 mg/kg). For EEG recording, two stainless steel miniature screw electrodes were implanted in the skull (1.0 mm anterior to the bregma, 1.0 mm to the right of the midline; 2.5 mm posterior to the bregma, 2.5 mm to the left of the midline). Teflon-coated stainless steel wires were implanted in the neck muscles on both sides to record an electromyogram (EMG). A telemetric device (TA10TA-F20; Data Sciences Int., USA) to record body temperature (BT) and locomotor activity was implanted in the peritoneal cavity.

2.3. Sleep data analysis

Offline sleep scoring was performed on the computer screen by visual assessment of EEG and EMG activity using the Spike2 analysis program (CED, Cambridge, UK). Vigilance states were based on data binned in 6-second epochs and classified as wakefulness, rapid eye movement (REM) or NREM sleep. NREM sleep was characterized by continuous, slow, high-voltage EEG and low-voltage EMG activity. REM sleep was characterized by low-voltage EEG with continuous theta waves and total suppression of EMG. The EEG power spectrum in the epoch determined to represent NREM sleep was calculated by fast Fourier transform using the Spike2 analysis program. The EEG delta frequency band was set at 0.5–4.0 Hz. The delta power was normalized as a percentage of the total power (0.5–50 Hz) to calculate SWA. BT, locomotor activity, time spent sleeping and awake, and SWA were averaged over hourly intervals. A single cosine wave was fitted by a least squares method for each mouse to evaluate the acrophase (determined as a peak position of the cosine wave) for the sleep/wake pattern, BT, and locomotor activity rhythms. The implantable transmitters are unable to provide mean speed and thus locomotor activity in the present study means “relative activity”.

2.4. Procedure for baseline sleep recording

Mice (WT: $n = 5$, KO: $n = 5$) were individually housed after surgery until the end of the experiment. After two weeks of recovery from surgery, 10-week-old mice were transferred to plastic cages (20 × 24 × 30 cm) in a soundproof recording room and allowed to acclimate for 2 days. Flexible cables connected the mice to a polygraph and a computer-assisted data acquisition system (CED 1401 data processor, CED, Cambridge, UK). After the adaptation period, polygraphic recordings of EEG/EMG, BT and locomotor activity were made continuously for 24 h under a 12/12-hour L/D cycle.

2.5. Procedure for sleep recording under food deprivation (FD)

A separate group of mice (WT: $n = 6$, KO: $n = 6$) were used in the FD experiment. As with baseline recording, the mice were housed individually from surgery until the end of the recording. After 2 weeks of recovery from surgery, 10-week-mice were allowed to acclimate for 2 days in cages in a recording room. Polygraphic recordings of EEG/EMG, BT and locomotor activity were made continuously for 48 h under a 12/12-hour L/D cycle. Within this 48-hour period, sleep was recorded under ad libitum-fed control (CNT) conditions for the first 24 h. All food pellets were carefully removed from the recording cages at the start of the next day's light phase (zeitgeber time (ZT) 0), and sleep was recorded over the remaining 24 h.

2.6. Surgery and recording for cardiovascular data

Arterial pressure (AP) and heart rate (HR) were recorded in a separate group, which contained a minimal number of mice (WT: $n = 3$, KO: $n = 3$) because the cardiovascular recording device requires a more invasive implantation procedure than the sleep recording device. Mice were anesthetized with a cocktail of ketamine (100 mg/kg) and xylazine (25 mg/kg) for the implantation of a telemetric device. The tip of a catheter of a telemetric device for AP (TA11PA-C20; Data Sciences International, St. Paul, MN) was inserted into the aortic arch via the left carotid artery, with the telemeter body positioned subcutaneously on the right flank. Offline analysis was carried out on a computer with the Spike 2 program (CED, Cambridge, UK). The mean AP was calculated as the average of the digitized AP signal in consecutive 1-second epochs, and the HR was detected from the AP signal. For observation of the diurnal features of mean AP and HR, the mean AP and HR were averaged every 4 h for each animal.

As in the case of sleep recording, mice were housed individually from surgery until the end of the recording. After 2 weeks of recovery from surgery, 10-week old mice were allowed to acclimate for 2 days in cages in a recording room. The mean AP and HR were recorded continuously for 48 h under a 12/12-hour L/D cycle. For the cardiovascular recording, the mice used for baseline recording were also used for FD experiments. Within this 48-hour period, mean AP and HR were recorded under ad libitum-fed conditions for the first 24 h (baseline and CNT). All food pellets were carefully removed from the recording cages at the start of the next day's light phase (ZT0), and mean AP and HR were recorded over the remaining 24 h (FD).

2.7. Real-time RT-PCR analysis

For biochemical analysis, 24 mice (WT–CNT: $n = 6$, KO–CNT: $n = 6$, WT–FD: $n = 6$, KO–FD: $n = 6$) were used. WT–CNT and KO–CNT mice were fed ad libitum, while WT–FD and KO–FD mice were food deprived from ZT0 to the end of tissue sampling (ZT22–23). Mice were euthanized between ZT22 and ZT23 by rapid cervical dislocation. Tissues used for molecular analysis were dissected immediately after decapitation, frozen in liquid nitrogen, and stored at –80 °C until use. Total RNA was isolated from the liver, hypothalamus, and cortex following Takara's RNA isolation protocol (RNAisoPlus; Takara Bio, Shiga, Japan). cDNA was generated from each tissue RNA sample using a High-Capacity cDNA Transcription Kit (Applied Biosystems, Foster, CA, USA). We used predesigned, gene-specific TaqMan probes and primer sets (Applied Biosystems, Foster City, CA) to assess the gene expression of Hmgcs2 (Mm00520236_m1). Real-time RT-PCR was carried out using a StepOnePlus™ real-time PCR system (Applied Biosystems) and TaqMan universal PCR Master Mix (Roche Applied Science, Mannheim, Germany) according to the manufacturer's instructions. For endogenous

quantity control, we normalized values to those for the housekeeping gene *β-actin* (Mm00607939_s1).

2.8. Measurement of plasma levels of glucose, triglycerides, free fatty acids (FFAs), and ketone bodies

Trunk blood was collected for measurement of glucose, triglyceride, FFA, and ketone body (acetoacetate and β-hydroxybutyrate) levels. Whole blood samples containing EDTA–2Na (1 mg/ml) were centrifuged at 4 °C to separate out the plasma. Plasma glucose, triglyceride, and FFA levels were determined by HK-UV (glucose), GPOHDAOS (triglycerides), and ACS-ACOD (FFAs) enzyme assays using an automatic biochemical analyzer system (HITACHI 7180, Hitachi, Tokyo, Japan and JCA-DM2250, JEOL, Tokyo, Japan). Ketone bodies were measured by an automatic analyzer system JCA-BM12 (JEOL, Tokyo, Japan) using reagents for the measurement of ketone bodies by enzymatic assay (Kainos Laboratories, Tokyo, Japan).

2.9. Statistics

The results are expressed as the means ± SEM. Statistical analysis was carried out using the software package SPSS (SPSS Inc., Chicago, IL, USA). For comparisons between 2 groups (WT vs KO mice) at baseline, repeated-measures two-way analysis of variance (ANOVA) and Student's *t*-test (Figs. 1 and 2) were used. For the experiment using the FD paradigm, changes in sleep architecture, SWA, BT, locomotor activity, mean AP and HR were analyzed by one-way ANOVA followed by Tukey's post hoc test (Figs. 3 and 4). Plasma and real-time RT-PCR data were analyzed using Student's *t*-test (Fig. 5). $P < 0.05$ was assumed to indicate statistical significance.

3. Results

3.1. Sleep/wake pattern in PPARα KO mice at baseline under ad libitum-fed conditions

PPARα KO mice showed no major change in the amount of sleep or wakefulness under ad libitum fed conditions (effect sizes: wakefulness, genotype $\eta_p^2 = 0.119$, genotype × time $\eta_p^2 = 0.154$; NREM, genotype $\eta_p^2 = 0.112$, genotype × time $\eta_p^2 = 0.158$; REM, genotype $\eta_p^2 = 0.021$, genotype × time $\eta_p^2 = 0.125$) (Fig. 1A–C). KO mice showed significantly greater SWA during NREM sleep, especially from the late half of the light phase to the early half of the dark phase, than WT mice (genotype $\eta_p^2 = 0.412$, genotype × time $\eta_p^2 = 0.179$) (Fig. 1D). The EEG waveform (Fig. 1E) and power spectrum (Fig. 1F) of KO mice in NREM sleep also showed greater SWA than those of WT mice, suggesting that KO mice were sleepier.

In order to evaluate circadian rhythm of each sleep parameters, acrophase was calculated by the single cosinor technique (fitting a 24-hour cosine curve to all data by least squares linear regression). Although the acrophase (time of the peak in the fitted cosine curve) of rhythm for wakefulness and NREM sleep tended to be delayed approximately 1.5 h in PPARα KO mice in comparison with that in WT mice, these delays were not significant (effect sizes: wakefulness, $r = 0.60$; NREM, $r = 0.60$) (Fig. 1A and B). However, the acrophase of the rhythm for SWA during NREM sleep was significantly delayed by approximately 2 h in KO mice in comparison with that in WT mice ($r = 0.83$) (Fig. 1D).

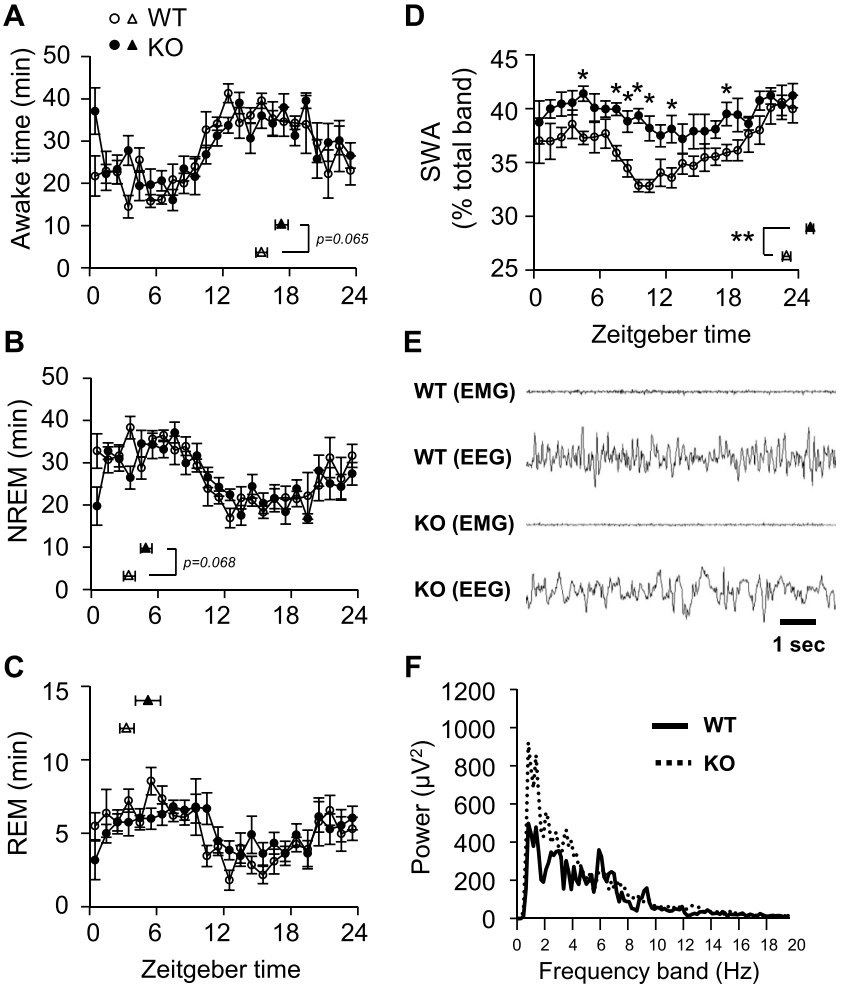

Fig. 1. Comparison of sleep/wake patterns in wild-type (WT) and peroxisome proliferator-activated receptor alpha (PPARα) knockout (KO) mice at baseline under ad libitum-fed conditions. Hourly time course for wakefulness (awake time) (A), non-rapid eye movement (NREM) sleep (B), rapid eye movement (REM) sleep (C), and slow-wave activity (SWA) during NREM sleep (D). Triangles in the line graphs indicate the acrophase in each parameter. Open circles and triangles indicate WT mice, while closed circles and triangles indicate KO mice. (E) Representative electromyogram (EMG) and electroencephalogram (EEG) showing SWA during NREM sleep in WT and KO mice. (F) Representative EEG power spectra during NREM sleep in WT and KO mice at ZT11. The solid line indicates WT mice, and the dashed line indicates KO mice. All data are expressed as the means ± SEM (A–D, $n = 5$/group). $^*p < 0.05$, $^{**}p < 0.01$, WT versus KO mice.

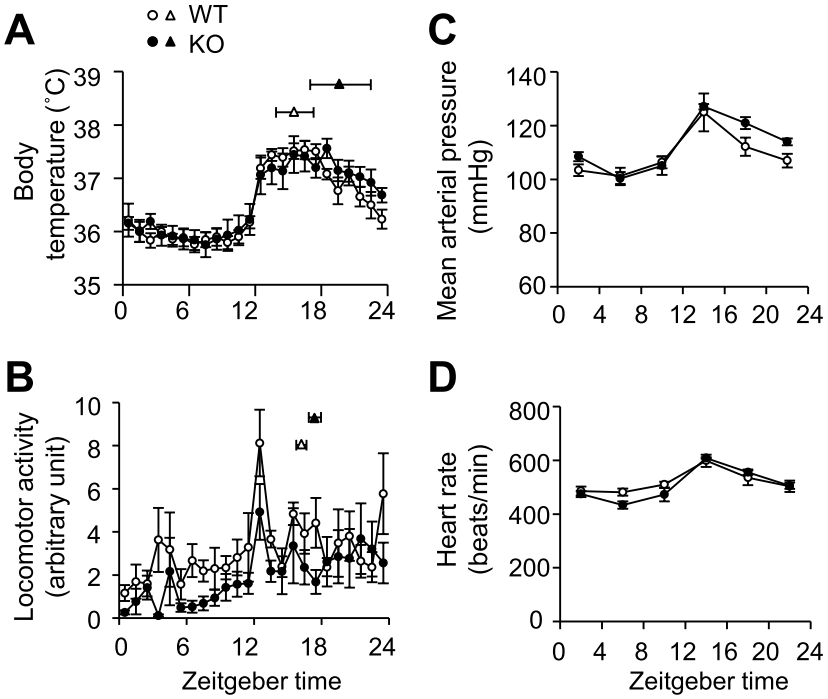

Fig. 2. Changes in body temperature (BT), locomotor activity and the cardiovascular system of wild-type (WT) and peroxisome proliferator-activated receptor alpha (PPARα) knockout (KO) mice at baseline under ad libitum-fed conditions. Hourly time course for BT (A) and locomotor activity (B). Triangles in the line graphs indicate the acrophase in each parameter. Time course of every four hours for mean arterial pressure (AP) (C) and heart rate (HR) (D). Open circles and bars indicate WT mice, and closed circles and bars indicate KO mice. All data are expressed as the means ± SEM (A and B, n = 6/group; C and D, n = 3/group).

3.2. BT, locomotor activity, mean AP and HR at baseline under ad libitum-fed conditions

There was no significant difference in BT between PPARα KO and WT mice (genotype η_p^2 = 0.011, genotype × time η_p^2 = 0.099) (Fig. 2A). Locomotor (relative) activity analysis revealed that KO mice tended to exhibit less locomotor activity during the light phase than WT mice, but the difference was not significant (genotype η_p^2 = 0.208, genotype × time η_p^2 = 0.073) (Fig. 2B). There was no significant difference in mean AP or HR between WT and KO mice under ad libitum-fed conditions (AP, genotype η_p^2 = 0.347, genotype × time η_p^2 = 0.229; HR, genotype η_p^2 = 0.073, genotype × time η_p^2 = 0.402) (Fig. 2C and D).

3.3. Sleep/wake pattern in PPARα KO mice during FD

At the beginning of the light phase (ZT0-4) of the FD day, both food-deprived WT and KO mice showed increased amounts of wakefulness and decreased NREM sleep compared with mice in the ad libitum-fed (CNT) conditions (effect sizes: wakefulness, η^2 = 0.77; NREM, η^2 = 0.74) (Fig. 3A and B). At the beginning of the dark phase (ZT12-16) during the FD day, food-deprived WT mice showed increased amount of wakefulness, and food-deprived KO mice showed the same tendency (η^2 = 0.44) (Fig. 3A). However, at the end of the dark phase (ZT20-24) of the FD day, the amount of wakefulness of food-deprived KO mice was markedly lower than that of food-deprived WT mice or ad libitum-fed KO mice, while that of food-deprived WT mice was not altered (η^2 = 0.70) (Fig. 3A). Consistent with these results, a significant increase in the amount of NREM sleep at the end of the dark phase (ZT20-24) of the FD day was observed in food-deprived KO mice but not in food-deprived WT mice (η^2 = 0.73) (Fig. 3B). The amount of REM sleep was lower in the FD condition than in the CNT condition in both WT and KO mice, especially at the beginning of the dark phase (ZT12-16) (η^2 = 0.59) (Fig. 3C).

SWA during NREM sleep reproduced the baseline results shown in Fig. 1; ad libitum-fed KO mice showed a greater SWA compared with that of ad libitum-fed WT mice under the CNT condition (ZT0-4, η^2 = 0.63; ZT4-8, η^2 = 0.60; ZT8-12, η^2 = 0.66; ZT12-16, η^2 = 0.74; ZT16-20, η^2 = 0.50; ZT20-24, η^2 = 0.66) (Fig. 3D). However, under the FD condition, the SWA of food-deprived WT mice tended to be enhanced, while that of food-deprived KO mice tended to be attenuated, and the difference between the two genotypes was smaller than under the CNT condition (Fig. 3D).

3.4. BT, locomotor activity, mean AP and HR during FD

BT was markedly lower in the middle and end of the dark phase of the FD day than under CNT conditions in both WT and PPARα KO mice (ZT16-20, η^2 = 0.89; ZT20-24, η^2 = 0.93) (Fig. 4A). FD increased locomotor (relative) activity at the beginning of the dark phase (ZT12-16) only in food-deprived WT mice (η^2 = 0.40) (Fig. 4B). On the other hand, FD induced a significant decrease in locomotor activity at the end of the dark phase (ZT20-24) only in food-deprived KO mice (η^2 = 0.44) (Fig. 4B). During the middle and end of the dark phase, the mean AP was decreased by FD only in KO mice, compared with ad libitum-fed KO mice and food-deprived WT mice (ZT16-20, η^2 = 0.80; ZT20-24, η^2 = 0.85) (Fig. 4C). HR was suppressed by FD in both WT and KO mice throughout the dark phase, but the decrease was larger in food-deprived KO mice than in food-deprived WT mice (ZT12-16, η^2 = 0.90; ZT16-20, η^2 = 0.94; ZT20-24, η^2 = 0.97) (Fig. 4D).

3.5. Ketone bodies in PPARα KO mice

To determine the cause of sleep changes in PPARα KO mice, we next measured plasma concentrations of glucose, triglycerides, FFA, and ketone bodies (acetoacetate [AcAc] and β-hydroxybutyrate [BHB]). Under CNT conditions, there was no difference in plasma glucose level between the genotypes, although the glucose levels of the KO mice tended to be higher than those of the WT mice (effect size: r = 0.55) (Fig. 5A). After FD, glucose levels decreased in both WT and KO mice, but the decline in KO was more pronounced (r = 0.93) (Fig. 5A). The plasma triglyceride concentration was increased in KO mice under both the CNT and FD conditions (CNT, r = 0.76; FD, r = 0.69) (Fig. 5B). The increase in FFA after FD was greater in KO mice than in WT mice (r = 0.80) (Fig. 5C).

Analysis of ketone bodies revealed that peripheral plasma AcAc levels were significantly higher in KO mice than in WT mice under CNT conditions, while BHB levels were significantly lower (AcAc, r = 0.67;

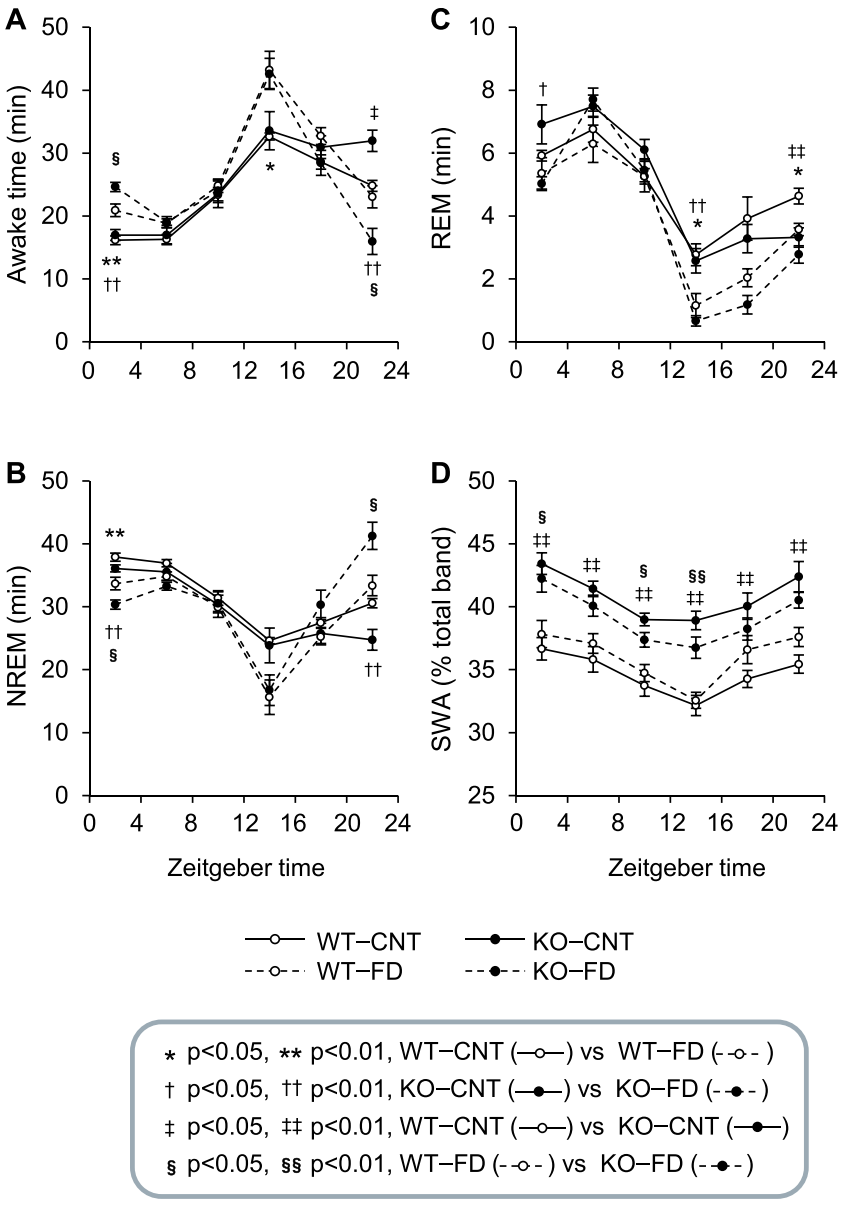

Fig. 3. Sleep/wake patterns in wild-type (WT) and peroxisome proliferator-activated receptor alpha (PPARα) knockout (KO) mice during food deprivation (FD). Time courses of wakefulness (awake time) (A), non-rapid eye movement (NREM) sleep (B), rapid eye movement (REM) sleep (C), and slow-wave activity (SWA) during NREM sleep (D) in WT and KO mice, presented in four-hour increments. Open circles with a solid line indicate ad libitum-fed WT mice (WT − CNT), open circles with a dashed line indicate food-deprived WT mice (WT − FD), closed circles with a solid line indicate ad libitum-fed KO mice (KO − CNT), and closed circles with a dashed line indicate food-deprived KO mice (KO − FD). All data are expressed as the means ± SEM (n = 6/group).

BHB, r = 0.76) (Fig. 5D and E). Plasma AcAc and BHB levels in KO mice, compared with those in WT mice, showed an attenuated increase when mice were subjected to FD (AcAc, r = 0.65; BHB, r = 0.88) (Fig. 5D and E). In KO mice, the peripheral plasma ketone body ratio (AcAc/BHB) was significantly higher than in WT mice both under CNT and FD conditions (CNT, r = 0.94; FD, r = 0.93) (Fig. 5F).

The mRNA expression of Hmgcs2 (a target gene of PPARα and the rate-limiting gene for ketogenesis in mitochondria) in both the hypothalamus and the cortex was significantly lower in KO mice than in WT mice under ad libitum-fed conditions (hypothalamus, r = 0.89; cortex, r = 0.68) (Fig. 5H and I). FD induced a marked increase in the mRNA expression of Hmgcs2 in the liver, hypothalamus and cortex in WT mice, while these increases were attenuated in KO mice, especially in the liver and hypothalamus (liver, r = 0.91; hypothalamus, r = 0.90) (Fig. 5G, H and I).

4. Discussion

Behavioral and metabolic adaptation is essential for survival during FD. In the present study, the effect of the energy shortage, i.e., the energy-saving response caused by FD, seemed to emerge in the dark phase. In particular, at the end of the dark phase (ZT20-24) when the duration of FD exceeded 20 h, the difference in sleep parameters between WT and PPARα KO mice became very prominent. In food-deprived WT mice, increased wakefulness and locomotor activity were observed at the beginning of the dark phase (ZT12-16) of the FD day, but both variables returned to the CNT level at the end of the dark phase (Figs. 3A and 4B, ZT20-24). On the other hand, in food-deprived KO mice, waking time and locomotor activity were markedly decreased, and the amount of NREM sleep was greatly increased at the end of the dark phase (Figs. 3A, B and 4B, ZT20-24). These results indicate that PPARα is required to maintain arousal during 24-hour FD.

As shown in previous studies, fasting and food restriction caused a large decrease in BT, AP and HR in mice [19]. In our study, FD that began at the beginning of the light phase induced a significant drop in BT during the middle and end of the dark phase in both WT and PPARα KO mice (Fig. 4A). On the other hand, the responses of mean AP and HR to FD were markedly different between WT and KO mice. The mean AP and HR of food-deprived KO mice declined more steeply than those of food-deprived WT mice at the end of the dark phase (Fig. 4C and D, ZT20-24). These results indicate that PPARα is involved in the regulation of cardiovascular function when FD lasts sufficiently long.

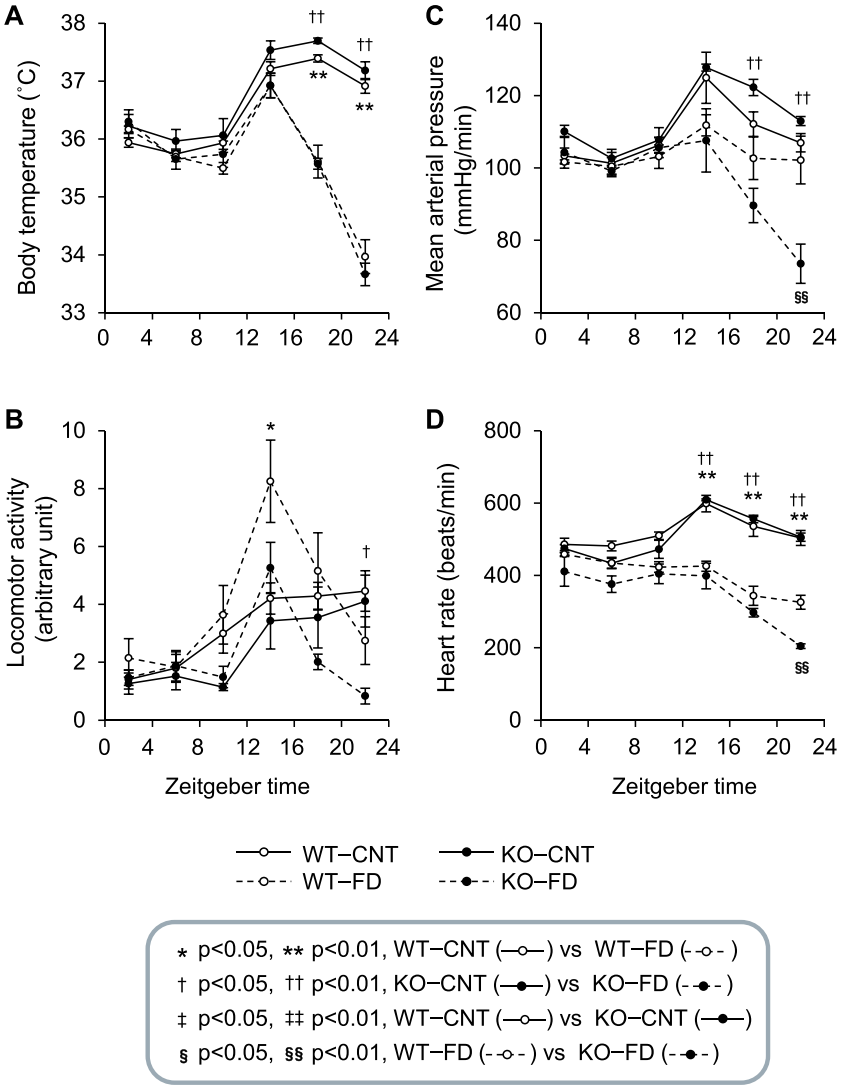

Fig. 4. Changes in body temperature (BT), locomotor activity and the cardiovascular system of wild-type (WT) and peroxisome proliferator-activated receptor alpha (PPARα) knockout (KO) mice during food deprivation (FD). Time courses of BT (A), locomotor activity (B), mean arterial pressure (AP) (C) and heart rate (HR) (D) in WT and KO mice, presented in four-hour increments. Open circles with a solid line indicate ad libitum-fed WT mice (WT − CNT), open circles with a dashed line indicate food-deprived WT mice (WT − FD), closed circles with a solid line indicate ad libitum-fed KO mice (KO − CNT), and closed circles with a dashed line indicate food-deprived KO mice (KO − FD). All data are expressed as the means ± SEM (A and B, n = 6/group; C and D, n = 3/group).

Although especially notable in PPARα KO mice, an FD-induced drop in HR was also observed in WT mice at the beginning of the dark period (Fig. 4D). Despite this decrease in HR, wakefulness and locomotor activity were both increased at the beginning of the dark phase in WT, while the corresponding change in KO mice was not significant (Figs. 3A and 4B). FD is well known to increase the amount of wakefulness with increased food-seeking behavior [20–22]. Because an increase in food seeking during FD is essential to survival, it may overwhelm the suppression of physiological function under conditions of FD in WT mice. Enhanced wakefulness and food seeking at the beginning of the dark phase as a result of FD may also be partially moderated by PPARα.

Ketone bodies, such as AcAc and BHB, are generated from the breakdown of fatty acids and become major fuels in most tissues during starvation, prolonged exercise, or consumption of a high-fat diet [23,24]. Although the liver is generally considered to be the main organ supplying ketone bodies, astrocytes in the brain also produce ketone bodies from fatty acids [25,26]. Ketogenesis is modulated by the activity of PPARα and its target gene *Hmgcs2* [1,27]. During fasting, the brain switches from the use of glucose to the use of ketone bodies [28]. A similar mechanism has been observed in the heart, in which fasting induces a transition to ketone body utilization from FFA to provide an alternative fuel source for the myocardium [29,30]. In the present study, PPARα KO mice showed fewer ketone bodies (AcAc and BHB) than WT mice during FD because of decreased mRNA expression of Hmgcs2, a target gene of PPARα and a rate-limiting enzyme of ketogenesis, in the liver and the hypothalamus (Fig. 5D, E, G and H). This reduction in ketone bodies in PPARα KO mice may lead to the loss of an energy source for the heart and brain, causing the decreases in AP, HR, and wakefulness observed at the end of the dark phase of the FD day.

As mentioned above, sleep measurements were dramatically altered by PPARα deficiency under the FD condition. On the other hand, under the ad libitum-fed condition, only SWA during NREM sleep differed between the two genotypes, while the other sleep parameters, including the duration of sleep, were similar in WT and PPARα KO mice. PPARα is involved in sleep quality, and our previous study demonstrated that mice treated with bezafibrate, a PPARα agonist, showed enhanced SWA in NREM sleep, an indicator of sleep depth and sleepiness [14]. Unexpectedly, in this study, PPARα KO mice also showed enhanced SWA in NREM sleep compared with WT mice at baseline (Fig. 1D–F). The exact reason for this discrepancy is unknown at this point but may be partly explained by the association with the ketone bodies. In our previous study, mice treated with bezafibrate showed an increased AcAc and a decreased BHB plasma concentration, leading to an increased ketone body ratio (AcAc/BHB) [14]. In the present study, PPARα KO mice also showed increased AcAc, decreased BHB, and an increased ketone body ratio compared with WT mice under ad libitum-fed conditions, although the elevation in ketone bodies as a response to FD was attenuated (Fig. 5D–F). The ketone body ratio is reported to reflect the redox state (NAD^+/NADH) within the mitochondrial matrix

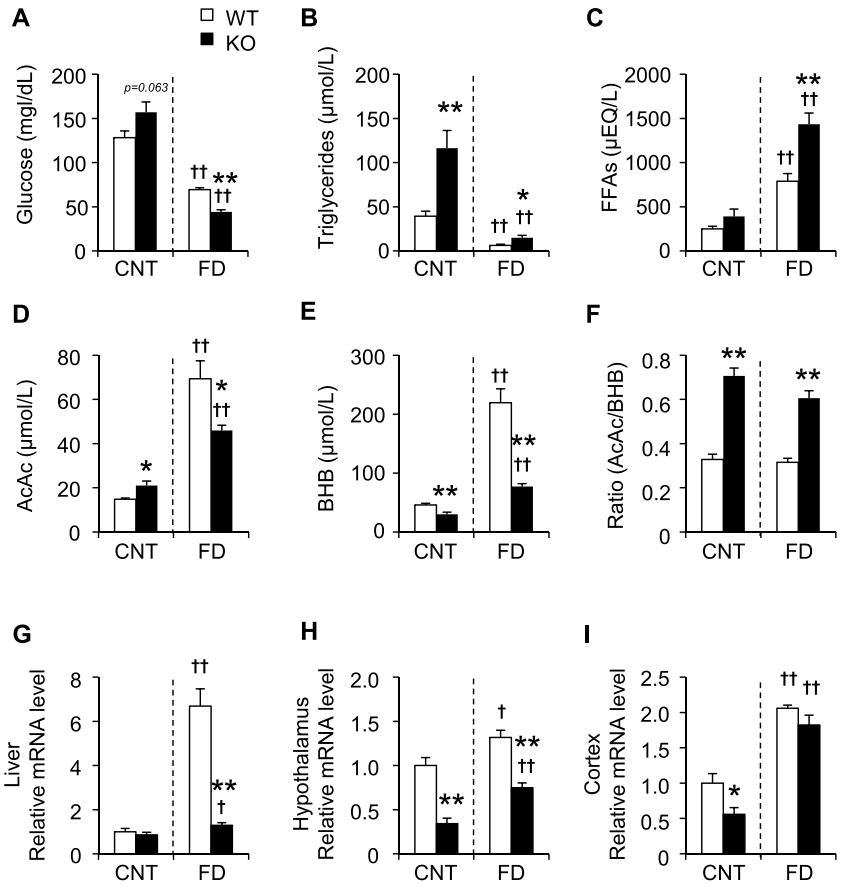

Fig. 5. Plasma concentration of biochemical substances and gene expression related to ketogenesis in wild-type (WT) and peroxisome proliferator-activated receptor alpha (PPARα) knockout (KO) mice during food deprivation (FD). Plasma concentrations of glucose (A), triglycerides (B), free fatty acids (FFAs) (C), acetoacetate (AcAc) (D), and β-hydroxybutyrate (BHB) (E) and the ketone body ratio (AcAc/BHB) (F) under ad libitum-fed (control, CNT) and FD conditions. Real-time RT-PCR analysis of mRNA expression of Hmgcs2 in the liver (G), hypothalamus (H), and cortex (I) under CNT and FD conditions. Open bars indicate WT mice, and closed bars indicate KO mice. All data are expressed as the means ± SEM (n = 5–6/group). $^{*}p < 0.05$, $^{**}p < 0.01$, WT versus KO mice. $^{\dagger}p < 0.05$, $^{\dagger\dagger}p < 0.01$, CNT versus FD.

[31,32]. We can hypothesize that mitochondrial function may be involved in the regulation of SWA in NREM sleep.

In addition, circulating AcAc suppresses glutamate release by suppressing the activity of vesicular glutamate transporters (VGLUTs), which leads to consequent suppression of excitatory neurotransmission [33]. Glutamate is well known to be involved in sleep/wake regulation, and the glutamatergic projections are important for the awakening system [34]. In our previous study, mice centrally injected with AcAc demonstrated increased SWA during NREM sleep, accompanied by decreased glutamate release in the brain [15]. These findings suggest that increased AcAc would induce an enhancement of SWA in NREM sleep in PPARα KO mice, at least under ad libitum-fed conditions, as well as in bezafibrate-treated mice.

In conclusion, under conditions of PPARα deficiency, prolonged FD induced a decreased amount of wakefulness and locomotor activity accompanied by a significant decline in AP and HR, provably via suppression of ketone body supply as fuel. These results suggest that PPARα and ketone bodies may play an important role in the maintenance of wakefulness under conditions of lack of energy supply (negative energy balance), such as fasting. Our findings provide additional evidence for an interaction between energy metabolism and sleep/wake regulation.

Author contributions

All authors are responsible for the study concept and design. S.C. planned most of the experiments. Y.K., S.C. and N.S. performed most of the experiments. T.S. and D.T. contributed to the data analysis. All authors discussed the results. Y.K., S.C., and H.S. wrote the first draft of the manuscript. All authors revised the manuscript and gave final approval for the submitted manuscript.

Acknowledgments

We thank Katsutaka Oishi for the generous gift of PPARα KO mice. This study was supported by a grant from JSPS KAKENHI; grant number JP18K11047.

References

[1] B. Desvergne, W. Wahli, Peroxisome proliferator-activated receptors: nuclear control of metabolism, Endocr. Rev. 20 (1999) 649–688.
[2] N Bougarne, et al., Molecular actions of PPARalpha in lipid metabolism and inflammation, Endocr. Rev. 39 (2018) 760–802.
[3] P. Lefebvre, G. Chinetti, J.C. Fruchart, B. Staels, Sorting out the roles of PPAR alpha in energy metabolism and vascular homeostasis, J. Clin. Invest. 116 (2006) 571–580.
[4] W Ahmed, et al., PPARs and their metabolic modulation: new mechanisms for transcriptional regulation, J. Intern. Med. 262 (2007) 184–198.
[5] S. Kersten, B. Desvergne, W. Wahli, Roles of PPARs in health and disease, Nature 405 (2000) 421–424.
[6] T Hashimoto, et al., Defect in peroxisome proliferator-activated receptor alpha-inducible fatty acid oxidation determines the severity of hepatic steatosis in response to fasting, J. Biol. Chem. 275 (2000) 28918–28928.
[7] S Kersten, et al., Peroxisome proliferator-activated receptor alpha mediates the adaptive response to fasting, J. Clin. Invest. 103 (1999) 1489–1498.
[8] T.C. Leone, C.J. Weinheimer, D.P. Kelly, A critical role for the peroxisome proliferator-activated receptor alpha (PPARalpha) in the cellular fasting response: the PPARalpha-null mouse as a model of fatty acid oxidation disorders, Proc. Natl. Acad. Sci. USA 96 (1999) 7473–7478.
[9] A. Cimini, M.P. Ceru, Emerging roles of peroxisome proliferator-activated receptors (PPARs) in the regulation of neural stem cells proliferation and differentiation, Stem Cell Rev. 4 (2008) 293–303.
[10] T Ouk, et al., Effects of the PPAR-alpha agonist fenofibrate on acute and short-term consequences of brain ischemia, J. Cereb. Blood Flow Metab. 34 (2014) 542–551.
[11] A Roy, et al., Regulation of cyclic AMP response element binding and hippocampal plasticity-related genes by peroxisome proliferator-activated receptor alpha, Cell Rep. 4 (2013) 724–737.
[12] S Chikahisa, et al., Enhancement of fear learning in PPARalpha knockout mice, Behav. Brain Res. 359 (2019) 664–670.
[13] E. Murillo-Rodriguez, The role of nuclear receptor PPARalpha in the sleep-wake cycle modulation. A tentative approach for treatment of sleep disorders, Curr. Drug

Deliv. 14 (2017) 473–482.
[14] S. Chikahisa, et al., Bezafibrate, a peroxisome proliferator-activated receptors agonist, decreases body temperature and enhances electroencephalogram delta-oscillation during sleep in mice, Endocrinology 149 (2008) 5262–5271.
[15] S. Chikahisa, N. Shimizu, T. Shiuchi, H. Sei, Ketone body metabolism and sleep homeostasis in mice, Neuropharmacology 79 (2014) 399–404.
[16] M. Grabacka, M. Pierzchalska, M. Dean, K. Reiss, Regulation of ketone body metabolism and the role of PPARalpha, Int. J. Mol. Sci. 17 (2016).
[17] T.A. Alvarenga, M.L. Andersen, L.A. Papale, I.B. Antunes, S. Tufik, Influence of long-term food restriction on sleep pattern in male rats, Brain Res. 1057 (2005) 49–56.
[18] N. Sato, S. Marui, M. Ozaki, K. Nagashima, Cold exposure and/or fasting modulate the relationship between sleep and body temperature rhythms in mice, Physiol. Behav. 149 (2015) 69–75.
[19] T.L. Jensen, M.K. Kiersgaard, D.B. Sorensen, L.F. Mikkelsen, Fasting of mice: a review, Lab Anim 47 (2013) 225–240.
[20] S. Chikahisa, et al., Histamine from brain resident MAST cells promotes wakefulness and modulates behavioral states, PLoS ONE 8 (2013) e78434.
[21] A. Yamanaka, et al., Hypothalamic orexin neurons regulate arousal according to energy balance in mice, Neuron 38 (2003) 701–713.
[22] N Goldstein, et al., Hypothalamic neurons that regulate feeding can influence sleep/wake states based on homeostatic need, Curr. Biol. 28 (2018) 3736–3747 e3733.
[23] T. Fukao, G.D. Lopaschuk, G.A. Mitchell, Pathways and control of ketone body metabolism: on the fringe of lipid biochemistry, Prostaglandins Leukot. Essent. Fatty Acids 70 (2004) 243–251.
[24] A.M. Robinson, D.H. Williamson, Physiological roles of ketone bodies as substrates and signals in mammalian tissues, Physiol. Rev. 60 (1980) 143–187.
[25] N. Auestad, R.A. Korsak, J.W. Morrow, J. Edmond, Fatty acid oxidation and ketogenesis by astrocytes in primary culture, J. Neurochem. 56 (1991) 1376–1386.
[26] C. Blazquez, C. Sanchez, G. Velasco, M. Guzman, Role of carnitine palmitoyltransferase I in the control of ketogenesis in primary cultures of rat astrocytes, J. Neurochem. 71 (1998) 1597–1606.
[27] T.E. Cullingford, The ketogenic diet; fatty acids, fatty acid-activated receptors and neurological disorders, Prostaglandins Leukot. Essent. Fatty Acids 70 (2004) 253–264.
[28] P. Puchalska, P.A. Crawford, Multi-dimensional roles of ketone bodies in fuel metabolism, signaling, and therapeutics, Cell Metab. 25 (2017) 262–284.
[29] N. Bouteldja, L.T. Andersen, N. Moller, L.C Gormsen, Using positron emission tomography to study human ketone body metabolism: a review, Metabolism 63 (2014) 1375–1384.
[30] M Bentourkia, et al., PET study of 11C-acetoacetate kinetics in rat brain during dietary treatments affecting ketosis, Am. J. Physiol. Endocrinol. Metab. 296 (2009) E796–E801.
[31] R.P Constantin, et al., Prooxidant activity of fisetin: effects on energy metabolism in the rat liver, J. Biochem. Mol. Toxicol. 25 (2011) 117–126.
[32] K. Katsuyama, K.M. Ozawa, S. Morikawa, S. Iwata, A. Mori, Myocardial high-energy phosphates and hepatic redox state in jaundiced rats, J. Surg. Res. 82 (1999) 88–94.
[33] N. Juge, et al., Metabolic control of vesicular glutamate transport and release, Neuron 68 (2010) 99–112.
[34] R.E. Brown, R. Basheer, J.T. McKenna, R.E. Strecker, R.W. McCarley, Control of sleep and wakefulness, Physiol. Rev. 92 (2012) 1087–1187.